Condensation of Vapor and Nanoclusters Formation within the Vapor Plume, Produced by ns-Laser Ablation of Si

B. S. Luk'yanchuk[*], **W. Marine** [**], **and S. I. Anisimov** [***]

[*]*General Physics Institute, Russian Academy of Sciences, Moscow, 117942 Russia*
E-mail: lukyanch@kapella.gpi.ru
[**]*UMR CNRS 6631, Faculte des Sciences de Luminy, Marseille, 13288 France*
E-mail: marine@gpec.univ-mrs.fr
[***] *L. D. Landau Institute for Theoretical Physics, Russian Academy of Sciences, Chernogolovka, 142432 Russia*
E-mail: anisimov@landau.ac.ru
Received August 7, 1997

Abstract - The condensation of vapor within the expanding plume produced by ns-laser ablation is discussed within the frame of Zeldovich and Raizer theory of condensation. The calculations have been done for the Si vapor. It is shown that the size of clusters formed during the condensation is very small because of fast expan-sion of the plume and quenching phenomena. The average cluster radius is calculated for different temperatures and densities of initial plume and it is typically of the order of few nanometers. The generalization of the theory is made for inhomogeneous plume where the rates of nucleation as well as condensation times are different for different parts of the plume. As a result, the distribution in cluster's size appears. Nevertheless, this distribution function is very sharp for the plume expanding in vacuum. For the clusters moving together with vapor one can distinguish three different waves propagating through the plume: (1) wave of saturation, where the vapor becomes saturated, (2) supercooling wave where the highest supercooling is reached, and (3) the quenching wave. Parameters for these waves are calculated. The possibility of oscillation phenomena during condensation is discussed.

1. INTRODUCTION

The physics of nanoclusters should be attributed to one of the most intensively developing branches of modern physics. The nanoclusters occupy an intermediate position between the quantum objects (atoms, molecules) and macroscopic objects, i.e., bulk materials. Thus, many properties of nanoclusters differ from both, the quantum objects and bulk materials. This is of great practical and scientific interest [1-3]. The fast development of this scientific brunch is caused by creation of reliable methods of cluster formation, including condensation of vapor during fast expansion of pulsed laser ablation products. The latter method permits to generate clusters of any materials with sizes typically by order of 10 - 1000 Å [1-6].

There is an important problem related to control of cluster size distribution produced by laser ablation. In an ideal situation it is desirable to form monosize clusters. with very narrow size distribution. Nevertheless it is not possible to do so for principal reasons – clusters of different sizes are forming during the expansion of inhomogeneous plume. The recent paper [7] considers that the distribution function arises due to cluster coalescence caused by collisions between the clusters. Thus, the authors of [7] modeled the cluster growth on the basis of Lifshitz - Slyozov theory (see, e.g. [8]).

Meanwhile, it is easy to estimate that for the typical conditions of nanosecond laser ablation of Si and evap-oration in vacuum, the collisions between clusters are very rare, and coalescence is unimportant. We have also mentioned that a long duration stage of very slow cluster growth exists before the coalescence stage. During this stage the distribution function is "frozen" (see, e.g. [9]).

Within the present paper we considers that coalescence is unimportant and discuss another effect related to the formation of distribution function due to the difference in condensation time in different parts of the plume. Roughly speaking, big clusters are formed within the center of the plume, while the smallest clusters are formed near the plume edge. For the theoretical analysis we used Zeldovich and Raizer (ZR) theory of condensation [10 – 12]. This theory refers to the initial stage of condensation process in contrast with Lifshitz - Slyozov theory which is applicable for the last stage of the condensation process (see, e.g. discussion in [8]).

An important part of the theory is the description of the nuclei production in supersaturated vapor. This description can be done on the basis of Zeldovich kinetic equation [10], which describes the production rate of overcritical nuclei (see also [8, 13]). Raizer [11] applied this kinetic equation (together with equation for the rate of droplets growth and the adiabatic equation in the condensation region) for the analysis of the problem of cosmic dust production during a collision (and further vaporization) of a large meteorite with the surface of a planet without an atmosphere. It was found that the degree of condensation, number of clusters and their size strongly depend on the velocity of the vapor expansion, which, in turn, depends on the initial size of the vapor,

evaporated mass, and internal energy. It was also shown in [11, 12] that condensation stops because of the quenching phenomenon.

Although ZR theory does not contain any fitting parameter, it is applicable (with small corrections) for the description of condensation within appreciably different conditions (it is sufficient to mention a tremendous difference, sixteen orders of magnitude, between evaporated mass in the case of the meteorite discussed in [11] and typical evaporated mass in laser ablation experiments and also a large difference in many other parameters).

Applying the ZR theory, we introduce a few corrections related to the peculiarities of the vapor plume produced in laser ablation experiments. First, we discuss the cooling rate of vapor, which is several orders of magnitude higher than in [11, 12]. Thus, all the important events (formation of the condensation region, production of nuclei, etc.) occur during the nonlinear stage of expansion, while in [11] calculations have been done for the linear stage (inertial expansion). For this reason, we discuss a more general description of the plume expansion.

Second, the nuclei produced in laser ablation plume have the size near the critical, $r \approx r_k$. Thus, it is necessary to include the influence of curvature into the equation for droplet growth. It was not very important in [11], where drops had a big size, $r \gg r_k$. We also made improvements in the procedure of the initial conditions calculation (initial condition for the droplet growth is not strictly defined within ZR theory).

The third correction refers to the estimation of the quenching time, $t = t_q$. In Raiser's paper [11] the criterium $q \, q / T \approx 1$ was used for this purpose, where q is supercooling, T is temperature, and q is the heat of vaporization (in Kelvin). The physical meaning of this criterium is a strong disturbance in thermodynamic "equilibrium" between the deposition and evaporation processes. We use another estimation, which shows the moment of time when the collisions stop within the expanding vapor. This criterium yields approximately 2.5 times higher value of t_q, but it does not influence strongly the final size of condensed droplets (difference smaller than 10 %). However, this difference can be easily detected experimentally (for example, with the help of time-of-flight mass spectroscopy [14]).

Raiser's examination was developed for homogeneous plume. It can be applied also to inhomogeneous plume under the assumption that the condensed droplets are moving together with vapor. This latter permits one to estimate the distribution function of condensed particles, which is done in the present paper.

The paper is organized as follows: We discuss the gas dynamics of the plume expansion in Section 2 and the mentioned modifications introduced within ZR theory in Sections 3-5. Then we analyze Si-nanoclusters formation within Si-vapor plume produced in vacuum by ns-laser ablation (Section 6). The main results of these studies are summarized in the conclusion (Section 7).

2. GAS DYNAMICS OF THE PLUME EXPANSION

Within the paper of Raizer [11] the simplified model of spherical plume expansion was used, namely, the averaged vapor density was taken in the following form:

$$r(t) = \frac{3M}{4pR^3} \quad , \quad R(t) = R_0 + ut \, , \qquad (1)$$

where M is the total mass of the vapor, R_0 is initial radius of the plume, and $u = \sqrt{2E / M} = const$ is the velocity of expansion, related to the initial internal energy E of the plume.

More accurate description can be made on the basis of the special solution of the gas dynamics equations (see, e.g. [15]), which yields the following law for isentropic expansion

$$\left(\frac{R}{R_0}\right)^2 = Y(t) \equiv 1 + 2\frac{u_0}{R_0}t + \left[\left(\frac{u_0}{R_0}\right)^2 + \frac{16}{3}\frac{E}{MR_0^2}\right]t^2. \qquad (2)$$

where u_0 is the initial velocity of the plume expansion. This solution holds for monatomic gas with adiabatic exponent $g = c_p / c_v = 5/3$. The general solution for arbitrary g is given in the Appendix.

At the later stages of expansion from (2) follows the linear law (inertial expansion). The density, specific volume, pressure and temperature profiles within the plume are given by

$$r(t) = r_0\left(1 - x^2\right)^{3/2} Y(t)^{-3/2}, \quad r_0 = \frac{8}{p^2}\frac{M}{R_0^3} \, , \qquad (3)$$

$$V(t) = V_0\left(1 - x^2\right)^{-3/2} Y(t)^{3/2}, \quad V_0 = \frac{p^2}{8}\frac{R_0^3}{M} \, , \qquad (4)$$

$$P(t) = P_0\left(1 - x^2\right)^{5/2} Y(t)^{-5/2}, \quad P_0 = \frac{128}{15p^2}\frac{E}{R_0^3}, \qquad (5)$$

$$T(t) = T_0\left(1 - x^2\right) Y(t)^{-1}, \quad T_0 = \frac{m}{R_g}\frac{16}{15}\frac{E}{M}, \qquad (6)$$

where $x = r / R(t)$ is the Lagrangian coordinate ($0 \leq x \leq 1$), R_g is the gas constant, and m is the atomic weight of the vapor.

We shall consider that small droplets of condensed vapor *move together with the vapor*. For this case, the condensation process can be discussed for each fixed

Lagrangian coordinate x independently. Here, we assume that the condensation process does change the expansion dynamics of the plume. For arbitrary value of x one can write the change of specific volume in the following form:

$$\frac{1}{V}\frac{dV}{dt} = \frac{3}{2}\frac{1}{Y}\frac{dY}{dt} \quad . \qquad (7)$$

This law will be used in the subsequent calculations.

3. THE SATURATION AND QUENCHING WAVES

The condensation process starts when the plume becomes saturated and stops when the plume starts to expand in collisionless (free-flight) regime. Within the inhomogeneous plume, saturation and free-flight regimes are reached for each point in different moments of time, i.e. saturation and quenching waves propagate through the expanding vapor.

Before the condensation starts, the expansion of the plume occurs along the Poisson adiabat, $PV^g = const$. It is convenient to write this equation in (V, T) coordinates, as $TV^{g-1} = const$. Thus, for monatomic gas

$$V = V_0\left[\frac{T}{T_0}\right]^{-3/2} \quad . \qquad (8)$$

This expansion continues up to the moment when the Poisson adiabat intersects the saturated vapor adiabat given by Clapeyron-Klausius equation [16]

$$P = P_s\left(\frac{T_s}{T}\right)^{1/2}exp\left[-\frac{q}{T}\right] , \qquad (9)$$

where q is the heat of vaporization given in Kelvin, $T_s = 300$ K, P_s is preexponential factor. This equation in (V,T) coordinates is given by

$$V = B\left(\frac{T}{T_s}\right)^{3/2}exp\left[\frac{q}{T}\right] , \qquad (10)$$

where $B = R_g T_s / mP_s$.

Condensation starts at the moment $t = t_c$, when the vapor is cooled up to the temperature $T = T_c$. This condensation temperature follows from (8) and (10). It is given by $T_c = qF(a)$, where $F(a)$ is the smaller root of the transcendental equation (the second, larger root, has no physical sense):

$$F^{-3}exp\left[-\frac{1}{F}\right] = a , \quad a = \frac{B}{V_0}\left(\frac{q^2}{T_sT_0}\right)^{3/2} . \qquad (11)$$

Parameter a is typically small, $à \ll 1$. This permits to write the approximate solution of (11) as

$$T_c \approx q\left\{ln\left(\frac{1}{a}\right)+3ln\left[ln\left(\frac{1}{a}\right)+3ln\;ln\left(\frac{1}{a}\right)\right]\right\}^{-1} . \qquad (12)$$
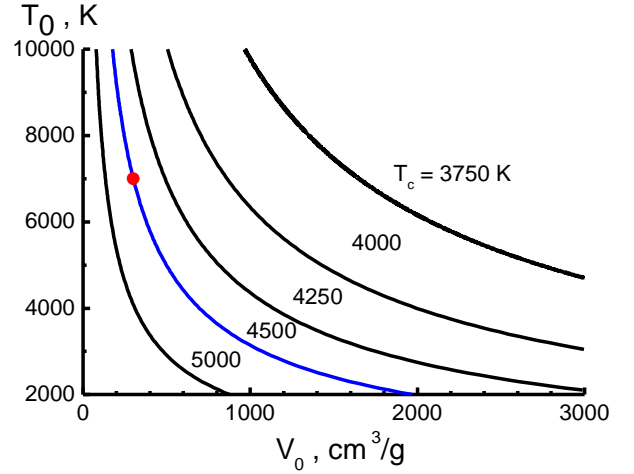
Fig. 1. Condensation isotherms T_c on the plane of parameters T_0, V_0.

It should be noted that T_c depends on initial parameters V_0 and T_0. At the same time it does not depend on Lagrangian coordinate x, i.e. we obtain the same con-densation temperature for different parts of the given plume. This condensation temperature T_c is shown in Fig. 1. Parameters of silicon [17] which have been used in calculations are presented in Table 1.

The moment t_c when condensation starts, depends on the Lagrangian coordinate, i.e. different parts of the plume start to condense at different moments. This moment of time can be found from the equation

$$Y(t_c) = \frac{T_0}{T_c}\left(1-x^2\right) . \qquad (13)$$

According to (13), the saturation wave propagates through the plume from its periphery to the center. The boundary of this wave $r = r_c(t)$ moves according to

$$\frac{r_c(t)}{R(t)} = \sqrt{1-\frac{T_c}{T_0}Y(t)} \quad . \qquad (14)$$

The plot of this function is shown in Fig. 2. We used for calculations the parameters of vapor given in Table 2.

Table 1. Parameters of Si [17], which have been used in calculations.

Parameter	Value
Density of condensed phase, r_c [g / cm^3]	2.4
Atomic weight, m [g / mole]	28
Heat of vaporization, q [K]	50615
Normalization temperature, T_S [K]	300
Preexponential factor, P_S [atm]	6.72×10^6
B, [cm^3 / g]	1.31×10^{-4}
Surface tension, s [erg / cm^2]	750
Cross-section of collisions, s_g [cm^2]	1.72×10^{-15}
Melting temperature, T_m [K]	1685
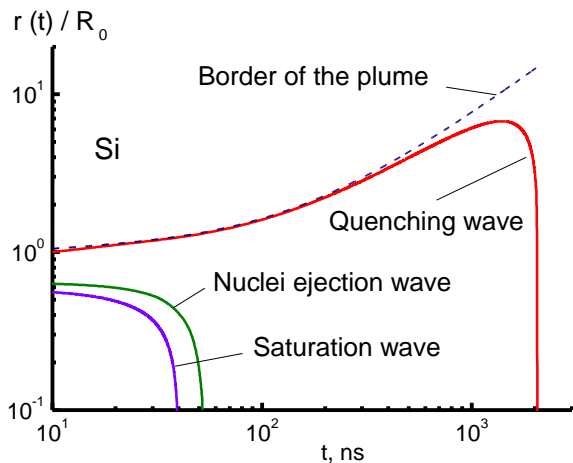
Fig. 2. Propagation of saturation, quenching and "ejection" waves through the Si-vapor plume with parameters of vapor given in Table 2.

Value of u_0 was measured experimentally [18]. For these parameters $T_c = 4500$ K (the corresponding point is shown in Fig. 1). Propagation of saturation wave strongly depends on initial velocity of the plume expansion, u_0 . For example, for $u_0 = 0$ saturation wave reaching point $r = 0$ (i.e. the whole plume becomes saturated) at the moment $t = 231$ ns, while for $u_0 = 6 \times 10^5$ cm/s this time is 40 ns. Also, we note that for the profiles given by (3) - (6), part of the plume with $r > 0.6 R_0$ is situated within the region of saturation from the initial moment of time, $t = 0$.

Now we should find the point of time when the condensation stops due to the so-called "quenching effect". It occurs because the collisions within the expanding vapor will stop at some stage of expansion (see more detail in [12]). A careful examination of this quenching effect needs the solution of Boltzmann kinetic equation.

We shall give the simplest estimation of this quenching time by a different way. Namely, to find the boundary $r = r_q(t)$ between the collision (hydrodynamic) and collisionless (free-flight) regions of the plume we use the criterium $\mathbf{l}\nabla v = v_s$. Here $\mathbf{l} = 1/s_g N = m/s_g$ $r(r)$ is the mean free path within the hydrodynamic region (s_g is cross-section of collisions), and v_s is the velocity of sound at the given point. The meaning of this

Table 2. Initial parameters of the plume, which have been used in calculations.

Initial parameters of the plume	Value
Initial temperature, T_0 [K]	7000
Initial specific volume, V_0 [cm^3/g]	300
Initial size, R_0 [cm]	0.1
Initial pressure, P_0 [atm]	68.4
Initial velocity of expansion, u_0 [cm/s]	6×10^5

criterium is rather simple. We consider that collisions exist until the neighbor particles (separated by $\mathbf{l}$ distance) is much less than the sound velocity (i.e., the mean molecular velocity). Substituting the value of the hydrodynamic velocity gradient, $\nabla v = \dot{R}/R = \frac{1}{2} Y^{-3/2} \frac{dY}{dt}$, and the sound velocity from

$$v_s(r) = \sqrt{\frac{5}{3}\frac{k_B T}{m}} = \sqrt{\frac{5}{3}\frac{k_B T_0}{m}} Y^{-1/2} \left(1 - \frac{r^2}{R^2}\right)^{1/2}, \quad (15)$$

we find the equation for the boundary of quenching wave

$$\frac{r_q}{R} = \sqrt{1 - \left(t_k Y \frac{dY}{dt}\right)^{1/2}}, \quad (16)$$

where

$$t_k = \frac{m V_0}{2 s_g} \sqrt{\frac{3}{5}\frac{m}{k_B T_0}} .$$

It can be seen from (16) and (2) that at $u_0 = 0$ the collisionless region spreads from the outer part of the plume $r = R_0$ (at $t = 0$). With $u_0 > 0$, the outer part of the plume spreads from the beginning in free-flight regime. Finally, at $u_0 > u_k = R_0 / 2 t_k$ the whole plume expands in collisionless regime. The critical velocity, u_k, is typically very high for developed ablation regime; however, it can be reached for subthreshold fluences whem the evaporated mass M is extremely small. Our calculations show the strong influence of the initial velocity u_0 on the quenching process. The whole plume becomes collisionless at $t = 5963$ ns with $u_0 = 0$ and at $t = 2071$ ns with $u_0 = 6 \times 10^5$ cm/s.

The propagation of the saturation and quenching waves through the plume is shown in Fig. 2. The picture is given in Euler's coordinates, the border of the expanding plume is shown in Fig. 2 as well. It can be seen from the figure that linear stage of the plume expansion starts at around 700 ns; thus, all important events within the plume occur during the nonlinear stage of expansion.

The third wave shown in Fig. 2 refers to the trajectory where the maximum of supersaturation is reached. At this condition the nuclei are formed ("ejected" into the saturated vapor). The equation for this wave will be obtained further on [see (37)].

4. THERMODYNAMICS OF TWO-PHASE REGION.

When the vapor becomes saturated and condensation starts, the matter within the plume is presented by two-phase system "liquid + vapor". One can denote the degree of condensation, x, as the ratio of the number density of molecules in the condensed phase to the total number density. If one supposes there is a thermodynamic equilibrium within the system, then the evolution of the system follows to equilibrium adiabat of

"two-phase" region. This adiabatic can be found from the equations ([11, 12]):

$$\left[c_V(1-x)+c_{\mathbf{l}}\,x\right]dT + \frac{R_g}{m}T(1-x)\frac{dV}{V}$$

$$= \left[\frac{R_g}{m}q-(c_{\mathbf{l}}-c_V)T\right]dx \qquad (17)$$

and

$$\frac{V}{(1-x)} = B\left(\frac{T}{T_s}\right)^{3/2}exp\left[\frac{q}{T}\right]. \qquad (18)$$

Equation (17) presents the energy balance for adiabatic process; here, c_v and c_l are the heat capacities of vapor (at constant volume) and liquid. For the problem under consideration one can put $c_v = 3R_g/2m$ and $c_l = 3R_g/m$. Equation (18) presents the saturation adiabat (10) where the specific volume of vapor is replaced by a specific volume of the original material. The system of equations should be solved together with initial condition

$$V\Big|_{T=T_c} \equiv V_c = B\left(\frac{T_c}{T_s}\right)^{3/2}exp\left[\frac{q}{T_c}\right] \qquad (19)$$

$$\text{or} \quad x\Big|_{T=T_c} = 0.$$

It is convenient to exclude specific volume V from (17)-(19) and introduce new variable: $y = q/T$ ($y_c = q/T_c$) instead of the temperature T. Then the problem under consideration is reduced to linear differential equation [19]

$$\frac{dx}{dy} + \frac{x}{y-1/2} = \frac{1-3/y}{y-1/2}, \quad x\Big|_{y=y_c} = 0. \qquad (20)$$

Integration of (20) yields the equilibrium degree of condensation within the vapor,

$$x_{eq} = \frac{2q}{2q-T}\left[\frac{T_c-T}{T_c} + 3\frac{T}{q}ln\left(\frac{T}{T_c}\right)\right]. \qquad (21)$$

One can find the adiabat of thermodynamically equilibrium two-phase system substituting (21) into (18),

$$V_{eq} = (1-x_{eq}(T))B\left(\frac{T}{T_s}\right)^{3/2}exp\left[\frac{q}{T}\right]. \qquad (22)$$

We denote the temperature along the equilibrium adiabat as equilibrium temperature T_{eq}. If the specific volume changes versus time according to (4), then the variation of equilibrium temperature $T_{eq}(t)$ can be found from (22):

$$V_0 Y^{\frac{3}{2}} = \left\{1-\frac{2q}{2q-T_{eq}}\left[\frac{T_c-T_{eq}}{T_c}+3\frac{T_{eq}}{q}ln\left(\frac{T_{eq}}{T_c}\right)\right]\right\}$$

$$\times B\left(\frac{T_{eq}}{T_s}\right)^{3/2}exp\left[\frac{q}{T_{eq}}\right] \qquad (23)$$

The variation of equilibrium degree of condensation is given by (21) where $x_{eq}(t) = x_{eq}[T_{eq}(t)]$. Using relation (7) one can rewrite the adiabatic equation (17) in the following form

$$(1+x)\frac{dT}{dt} + (1-x)\frac{T}{\Psi}\frac{d\Psi}{dt} = \left(\frac{2}{3}q-T\right)\frac{dx}{dt},$$

$$T\Big|_{t=t_c} = T_c. \qquad (24)$$

It is easy to see that the functions $T_{eq}(t)$ and $x_{eq}(t)$ ful-fill (24) automatically. Thus, for sufficiently slow expan-sion, when, according to thermodynamics, $x(t) \rightarrow x_{eq}(t)$, the evolution of the system occurs near the equilibrium phase trajectory defined by (22). For sufficiently fast expansion the phase trajectory can deviate from the equilibrium one. The similar phenomena can be seen quite often in nonequilibrium chemical kinetics [20].

One can see from (21) that at unrestricted vapor expansion, at the conditions close to equilibrium (i.e., when this expansion is realized rather slowly), the vapor should condense completely, $x_{eq}|_{T\rightarrow 0} \rightarrow 1$. At the case of fast expansion, the complete condensation does not occur due to quenching effect, i.e., $x \rightarrow x_q$, where $x_q < 1$.

The formal solution of (24) with $x = x_q = const$ yields the "quenching adiabate"

$$V = V_q\left[\frac{T}{T_q}\right]^{-\frac{3}{2}\left(\frac{1+x_q}{1-x_q}\right)}, \qquad (25)$$

which coincides with the Poisson adiabat with a renormalized adiabatic exponent. Thus, one can say that the quenching process goes along the Poisson quenching adiabat. However, this is rather formal, because the equation (24) is not valid to describe the collisionless vapor. It is more consequent to describe this effect in terms of "frozen temperature" T_q which corresponds to averaged kinetic energy of free-flight particles within the vapor.

In collisionless regime the clusters cooling rate is mostly determined by radiation heat loss. This cooling is quite fast for small clusters. For this situation, discussed further in calculations, the time necessary for cooling of 15 Å cluster from the quenching temperature $T_q = 2185$ K to the melting temperature T_m comprises $Dt \approx 370$ ns. It means that small clusters are deposited typically in solid state.

The equilibrium temperature $T_{eq}(t)$ (23) and the temperature $T = T_p(t)$ (6) are shown in Fig. 3 together with calculated temperature $T(t)$.

5. KINETICS OF CONDENSATION

According to (2) and (6) the cooling rate at the condensation point is given by

$$\frac{dT}{dt}\Big|_{t=t_c} = -(1-x^2)\frac{2T_c^2}{T_0}\frac{u_0}{R_0}\left(1+\frac{u_0 t_c}{R_0}+\frac{16}{3}\frac{Et_c}{MR_0 u_0}\right). \qquad (26)$$

Temperature, T, K

Supercooling, θ

Degree of condensation, x
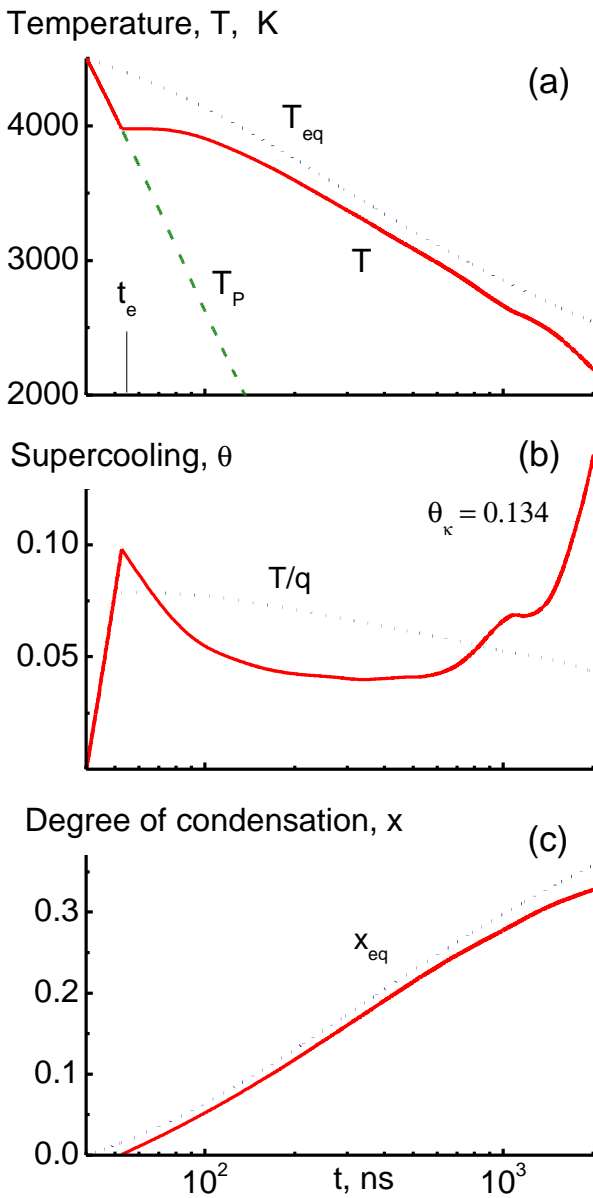
Fig. 3. Dynamics of the condensation process at adiabatic vapor expansion at $x = 0$: (a) Temperature $T(t)$ of Si-vapor. Symbol T_P denotes the temperature along the Poisson adiabat (6), and T_{eq} is the equilibrium temperature from equa-tion (23). (b) Supercooling $q = q(t)$ from calculations (solid line). The dotted curve presents dependence of T/q versus time. (c) Degree of condensation $x = x(t)$. Symbol x_{eq} denotes the equilibrium degree of condensation (21).

For the example shown in Fig. 3, this value is by order of 10^{11} K/s. It is evident that at such a high cooling rate vapor continues to expand during some time "by inertia" along the Poisson adiabat. As a result, vapor becomes oversaturated and the nucleation starts. Later the supersaturation drops because of the formation of critical nuclei and their further growth. The change of supersaturation is caused by the interplay between the rate of cooling (due to the work of vapor expansion) and the rate of heating (due to latent heat of condensation).

The condensation kinetics is governed by the value of supercooling (see, e.g., [12,13]):

$$q = \frac{T_{eq} - T}{T_{eq}} . \tag{27}$$

We can write now the kinetic equations assuming that for the given Lagrangian coordinate all the condensed clusters (nuclei) have the same size.

Let us consider that each cluster consists of $g = g(t)$ atoms. We denote $n = n(t)$ the number of condensation centers (per atom of vapor). Then the degree of condensation is given by

$$x(t) = n(t)\, g(t) . \tag{28}$$

Correspondingly, the rate of condensation can be presented as

$$\frac{dx}{dt} = g\frac{dn}{dt} + n\frac{dg}{dt} , \qquad x\Big|_{t=t_c} = 0 . \tag{29}$$

The first term in (29) describes the change of condensation due to the formation of nuclei, while the second one describes the change of condensation caused by cluster growth. Once again we emphasize that the equations (28), (29) are written for fixed Lagrangian coordinate.

The rate of nucleation can be described by solution of Zeldovich's kinetic equation [10]. The stationary solution of this equation (see, e.g. [8]) yields

$$\frac{dn}{dt} = k_n (1-x)\left(1-x^2\right)^{3/2} Y^{-3/2} exp\left[-\frac{T_n}{T}\frac{1}{q^2}\right], \tag{30}$$

$$n\Big|_{t=t_c} = 0 ,$$

where

$$k_n = \frac{r_0}{r_1}\, 4\sqrt{\frac{2s}{p\,m}} , \qquad T_n = \frac{16p\,s^3 m^2}{3k_B^3\, q^2\, r_1^2} . \tag{31}$$

Here, we use notation s for the surface tension. Preexponential factor in (30) is proportional to density of vapor. The equation (30) differs from the Raizer equation by factor $(1-x)\left(1-x^2\right)^{3/2} Y^{-3/2}$.

Ions may play an important role at the condition of high supercooling, $q > q_k$, where q_k is critical supercooling for charged particles [11]. At $q > q_k$ the charged complexes of all sizes exhibit a tendency to grow without limit. For Si $q_k = 0.134$. At $q \to 0$ the difference in nucleation of charged and uncharged particles disappears [11]. Thus, as a first approximation, one can neglect the influence of ionization onto the nucleation process (if q is smaller and not very close to q_k).

The equation for growth of cluster can be written under the assumptions used in [11] that the growth of

nuclei occurs in kinetically controlled regime, accommodation coefficient is equal to unity, and temperatures of gas and droplet are equal. Then

$$\frac{dg}{dt} = 4pr^2\left(j_d - j_e\right),\qquad(32)$$

where the flux of deposited atoms is given by $j_d = \frac{1}{4}nv_T$, $n = \frac{r}{m}$ is the number density of atoms in gas, $v_T = \sqrt{\frac{8k_BT}{pm}}$ is the arithmetic mean velocity (see, e.g. [21]).

The flux of evaporated atoms can be presented in the following form

$$j_e = n_1 v_1 \, exp\left[-\frac{q}{T}\left(1-\frac{r_0}{r}\right)\right],\qquad(33)$$

where v_1 is preexponential factor in evaporation law, $n_1 = \frac{r_1}{m}$ is the number density of atoms in condensed phase, term $\left(1-\frac{r_0}{r}\right)$ takes into account surface tension effect, $r_0 = \frac{2sw}{k_Bq}$, $w = m/r_1$ is the volume per atom in liquid. The radius of critical nucleus is given by $r_k = r_0/q$. For nucleus of critical size, the balance of evaporated and deposited fluxes should take place. This condition permits us to exclude factor n_1v_1 within the equation for droplet growth, which is transformed to

$$\frac{dg}{dt} = p \, r^2 n v_T \left[1 - \exp\left(-\frac{q}{T}q\left(1-\frac{r_k}{r}\right)\right)\right].\qquad(34)$$

This equation is different from the equation which has been used in [11] by general factor 1/4 (probably, misprinting) and factor $\left(1-\frac{r_k}{r}\right)$, which describes the difference in evaporation from spherical and flat surfaces. This factor was not very important in [11], where droplets had a big size $r \gg r_k$, but it is very important for the problem under discussion where sizes r and r_k are comparable.

Using $r = \left(\frac{3}{4p}\frac{mg}{r_1}\right)^{1/3}$ and formula (3) for the gas density we can rewrite (34) in the following form

$$\frac{dg}{dt} = k_g g^{\frac{2}{3}} \sqrt{T}\left(1-x\left(1-x^2\right)^{3/2}Y^{-3/2}\right.$$
$$\times\left\{1-exp\left[-\frac{q}{T}\left(q-ag^{-1/3}\right)\right]\right\}, \quad g\big|_{t=t_e} = g_0,\qquad(35)$$

where

$$k_g = \frac{pr_0}{m}\left(\frac{3}{4p}\frac{m}{r_1}\right)^{2/3}\sqrt{\frac{8k_B}{pm}},\; a = \frac{2sw}{k_Bq}\left(\frac{4p}{3w}\right)^{1/3}.\;(36)$$

The initial value of g_0 and "ejection time", t_e, should be found in a self-consistent way, using the assumption that cluster formation starts at the moment when supercooling reaches its maximum, and the smallest critical nuclei are ejected at this moment. Thus, $g_0 = g(t_e) = g_{min} = (a/q_{max})^3 \gg 1$, where g_{min} is the number of atoms within the smallest critical nuclei. Remember, that Zeldovich's kinetic equation considers g as a continuous variable, and applicable just for macroscopic description, i.e. $g \gg 1$.

To find time t_e we used the following procedure: During the initial stage, temperature T follows very close to Poisson adiabat $T = T_p(t)$, see (6), and one can put the supercooling $q_p = 1 - T_p(t)/T_{eq}(t)$. Degree of condensation is also very small, and one can neglect x within equation (24). The latter yields the moment t_e, when the super-cooling reaches extremum, $(dq/dt)\big|_{t=t_e} = 0$. This consideration yields the transcendental equation for t_e:

$$\frac{1}{T_{eq}}\frac{dT_{eq}}{dt} = -\frac{1}{Y}\frac{dY}{dt} + \left[\frac{2}{3}\frac{q}{T_p}-1\right]\left(\frac{a}{q_p}\right)^3\frac{dn}{dt}.\qquad(37)$$

The derivative (dn/dt) in (37) is taken along the Pois-son adiabat, $T = T_p$. For the given example, this equation yields for the center of the plume $t_e = 52.6$ ns and $g_{min} \approx 16.5$ atoms. The plot of the function $r = r(t_e)$ is shown in Fig. 2. It corresponds to the propagation of the "nuclei ejection" wave.

It is also convenient to recalculate the other initial conditions to the moment t_e:

$$T\big|_{t=t_e} = T_p(t_e), \quad g_0 = g(t_e) = g_{min},$$

$$n\big|_{t=t_e} = n_0 = \int_{t_c}^{t_e} \frac{dn}{dt}\bigg|_{T=T_p(t)}dt,\qquad(38)$$

and

$$x\big|_{t=t_e} = x_0 = g_0 n_0.$$

Thus, for the description of the condensation process we use the system of four ordinary differential equations for four unknown functions $T(t)$, $x(t)$, $n(t)$ and $g(t)$ together with corresponding boundary conditions at the point in time $t = t_e$.

6. NUMERICAL SIMULATION AND DISCUSSION

It should be noted that the "prehistory" of the system, for $t_c < t < t_e$, can not be described well by the model. Calculations with initial condition $g_0 < g_{min}$ show the dissociation of subcritical nucleus, while at $g_0 > g_{min}$ it starts to grow. At the limit case $g_0 = g_{min}$ we observed that an effect of the numerical instability perturbations pushed the system either into the dissociation or conden-

Number of clusters, ν, 10^{-4} (a)

Radius of cluster, r , A   (b)

Overcritical nuclei
$g_0 = g_{min} + 1.5$

r_k

Subcritical nuclei
$g_0 = g_{min} - 0.4$

t, ns
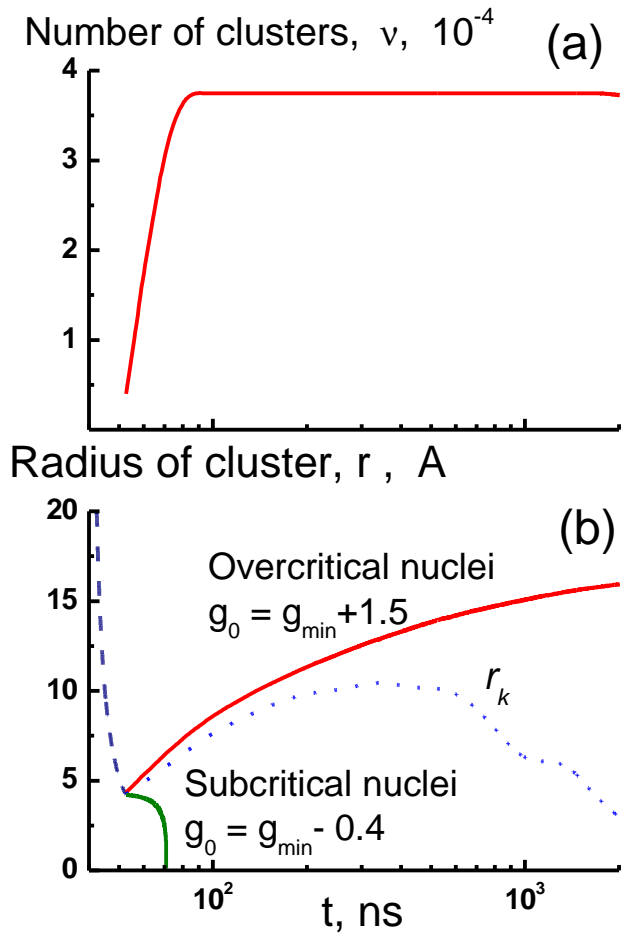
Fig. 4. Kinetics of condensation process at adiabatic vapor expansion. a) Number of clusters $n(t)$ per atom of Si vapor. b) Radius of growing cluster $r = r(t)$. Solid lines with $g_0 > g_{min}$ and $g_0 < g_{min}$ show the evolution of overcritical and subcritical nuclei, respectively. Symbol r_k denotes the critical radius for $g_0 > g_{min}$ (dotted line).

sation regions. In order to relieve these instabilities, and taking into account that the Zeldovich equation describes the production of slightly overcritical nuclei we use the following approximation: $g_0 = g_{min} + 1.5$, i.e. $g_0 = 18$ for $x = 0$.

The dynamics of the temperature $T(t)$, supercooling $q(t)$ and the degree of condensation $x(t)$ from numerical solution of the system is presented in Fig. 3. Integration was done with "Mathematica" software package [22]. The temperature $T(t)$ (Fig. 3a) firstly follows along the Poisson adiabat, then, after the start of nuclei formation it approaches the equilibrium temperature T_{eq}, and finally deviate from T_{eq} during the quenching. This behavior is typical for ZR theory.

Correspondingly, the supercooling (see Fig. 3b) reaches its first maximum at $t = t_e$, then it falls down, and finally increases up to the quenching time $t = t_q$. At final stage of condensation, the supercooling reaches its critical value q_k, where condensation on ions becomes dominant. It does not influence strongly the final size of nuclei, because it takes place within the region $qq/T > 1$. For the given example time t_R, which

corresponds to $qq/T = 1$, is ≈ 830 ns. As was mentioned above, this time $t = t_R$ was used in [11] as a criterion for stopping condensation. Strictly speaking, for $qq/T > 1$ the kinetic equation for droplet growth should be modified and the effects related to the difference in temperatures of the droplet and vapor should be taken into account. We have noted that this condition $qq/T > 1$ is also fulfilled at initial stage of the process (after nuclei ejection). A careful examination of the case $qq/T > 1$ needs solving of Boltzmann equation. The stationary solution of the problem was done in [23] but we did not find the general solution for the non-stationary situation.

Another important effect which can be seen in Fig. 3b is the oscillation in supercooling, which occurs at $t > 1000$ ns. This effect was not mentioned in [11], although the physics of this effect is rather simple. During the increase of supercooling, the rate of nuclei production and liberation of latent heat increase. At some conditions, the heat release may overcome cooling caused by the plume expansion. It leads to oscillation phenomena. These oscillations are very pronounced within certain region of parameters T_0 and V_0 (for example, at $T_0 = 9000$ K and $V_0 = 300$ cm^3/g). If the amplitude of these oscillations is sufficiently high, then a new portion of nuclei is ejected during the condensation. Their further growth leads to the production of clusters of different size. A detailed discussion of these oscillation effects in condensation will be published elsewhere.

Change of the degree of condensation, x, versus time is shown in Fig. 3c. It is shifted to the lower value compared to equilibrium one, $x < x_{eq}$. Although the final value, $x = 0.33$, is close to those obtained in [11] for iron meteorite ($x = 0.4$), there is a large difference in the number and size of clusters due to a significant difference in cooling rates. These characteristics for Si-vapor are shown in Fig. 4.

It can be seen from Fig. 4a that the number of clusters is practically a step-like function. Such behavior is in good agreement with the assumption that clusters within the vapor are practically of the same size (for the given Lagrangian coordinate). A cluster starts to grow from 17-atom nuclei and finally it contains approximately 880 atoms. For a comparison, the average number of atoms in the cluster which was found in [11] was $\approx 10^{10}$.

The radius of a growing cluster versus time is shown in Fig. 4b. From the figure we can see that a long stage of condensation occurs with $r \approx r_k$, where the effect of curvature is important. The final size of cluster for the given example is close to the minimal size of Si - clusters (diameter 1-3 nm), obtained experimentally at low *He* background gas pressure [4]. The resulting size of the forming cluster depends on the initial parameters of the plume, its mass, volume and temperature. The plots given in Fig. 5 illustrate the dependencies of the cluster size on the plume temperature and specific volume.
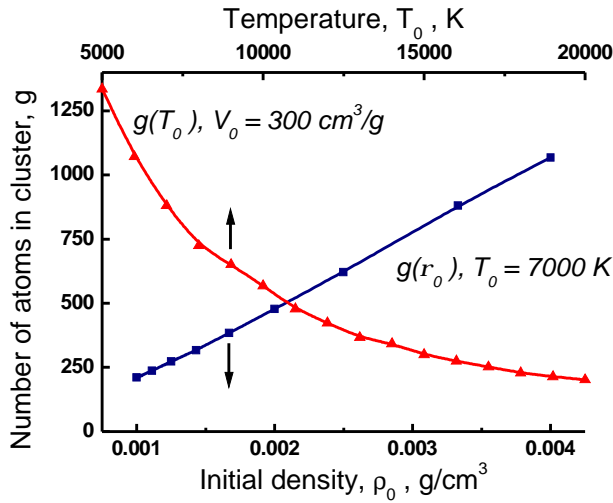
Fig. 5. Number of atoms within the cluster versus tempera-ture (triangles, upper axis)) and density squares, bottom axis).

Fig. 6. The normalized distribution function $f(r)$. Normalization corresponds to $\int_0^\infty f(r)dr = 1$.

Although one can see from the calculations that the cluster size falls down with an increase of the temperature (at fixed specific volume), it is difficult to realize this experimentally, for example, by a variation of laser parameters. Indeed, the increase of laser fluence leads to an increase of T_0 but it leads simultaneously to a decrease of V_0, i.e. the compensation effect takes place. Thus, to investigate the optimal laser control of the cluster formation one should solve the laser ablation problem (to find parameters T_0, V_0, etc.) together with the hydro-dynamic problem of vapor condensation.

In our calculations, we did not find any strong influence of the change of the surface tension, s, on the rate of cluster formation (this effect was mentioned in [7]). From our point of view, the drastic change of the rate of the cluster growth is related not to the surface tension value by itself but to the above-mentioned sensitivity of the growth kinetics to the initial conditions (see Fig. 4b). We should emphasize that during the size evolution, nuclei should overcome the "narrow throat" of critical size near the maximum of oversaturation.

The calculations given above were made for the center of the plume, $x = 0$. The calculations were performed by the same way for arbitrary Lagrangian coordinate. This calculation shows that the cluster size moving along the Lagrangian coordinate from the plume center to the plume edge decreases, while the number of clusters (per atom) increases. Thus, the degree of condensation from equation (28) varies slowly along x, but the decrease of the condensation also was obtained at the plume edge. To calculate dependencies $g(x)$ and $n(x)$ near the plume edge we use a smooth extrapolation of $g(x)$ and $n(x)$ by the best fitting cubic polynomial functions.
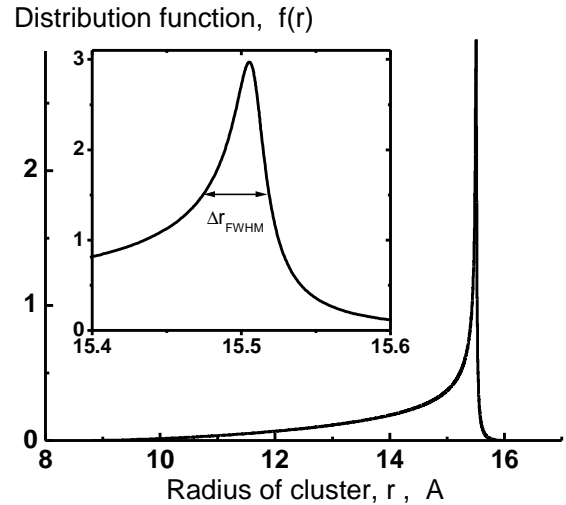
From $g(x)$ and $n(x)$ we plot the cluster size distribution function $f(r)$ (Fig. 6). The number of clusters produced within the interval dx is given by

$$dN = 4p\ \frac{r_0 R_0^3}{m}\left(1 - x^2\right)^{3/2} n(x)x^2 dx\ ,\qquad (39)$$

and variation in their size is $dr = \dfrac{dr}{dx}\,dx$. Thus, the distribution function can be defined as

$$F(r) = -\frac{dN}{dr} = -\frac{32}{p}\ \frac{M}{m}\frac{n(x)\,x^2\left(1 - x^2\right)^{3/2}}{dr/dx}\ .\quad (40)$$

Here, $dr/dx < 0$; thus, $F(r)$ is positive. This distribution function has the usual meaning: $F(r)dr$ shows the probability to find clusters with sizes between r and $r+dr$. The distribution function $F(r)$ is normalized to the total number of clusters, N, produced during the condensation:

$$\int_0^\infty F(r)dr = N = \frac{32}{p}\ \frac{M}{m}\int_0^1\left(1 - x^2\right)^{3/2} n(x)x^2 dx\ .\quad (41)$$

For the given example $N = 5\times10^{13}$ clusters. Instead of $F(r)$ we use the normalized distribution function, $f(r) = F(r)/N$. One can see from Fig. 6 that the obtained distribution function is extremely sharp. The half width at half maximum of the distribution function is $\Delta(2r)_{FWHM} \approx 0.1$ Å.

We have to note that in most of experimental works (e.g. [4, 6]) the distribution function of Si clusters shows a significant broadening. The high rate of Si clusters generation during these experiments was observed during laser ablation of silicon into the background gas, which change the expansion dynamics.

However, in our approach the distribution function also can be wider under the conditions when the pronounced oscillations in condensation take place or in the case of plume expansion into the surrounding media or in the case when the plume is asymmetrical (non-spherical). Analysis of these factors is out of the frame of the presented paper. We have only noted that the analysis of the asymmetrical 3D plume expansion can be done similarly to [24].

7. CONCLUSION

In this paper we discussed the peculiarities of fast condensation of vapor and nanocluster formation within the plume induced by pulsed laser ablation. The generalization of the Zeldovich-Raizer theory is done for inhomogeneous plume. The restrictions of the theory are discussed as well.

The calculations were made for Si-vapor plume produced at typical conditions of excimer ns-laser ablation. Results of the investigation can be summarized as follows:

(1) The typical cooling rate within the laser produced plume is very high, by the order of 10^{11} K/s. Thus, the main events in the condensation process (formation of the condensation region, production of nuclei, clusters growth) occur during the nonlinear stage of the plume expansion. This stage was described by the particular solutions of gas dynamics equations. Important parameters governing the expansion are initial plume size, total evaporated mass, internal energy, and initial velocity of expansion, u_0. In our calculations we used the experimental value $u_0 = 6\times10^5$ cm/s .

(2) Three waves propagate through the expanding plume: (a) wave of saturation, (b) supercooling wave, where the nuclei are ejected; and (c) the quenching wave, where the condensation stops. We found the basic equations for the propagation of these waves.

(3) At parameters used in calculations, clusters starts to grow from 18 atoms (within the critical nuclei) to 880 atoms as final, which corresponds to cluster diameter $\approx$ 30 Å. The significant stage of the cluster growth occurs near the critical radius; thus, effects related to nuclei curvature are very important. We show that the size distribution function of clusters is extremely sharp. For the spherical plume which expands into vacuum the half width at half maximum of the distribution function is $(2r)_{FWHM}$ $\approx$ 0.1 Å. The experimentally observed broadening of the size distribution function [4] is probably determined by the asymmetrical plume expansion.

The studies of the dependence of the cluster size versus the initial plume temperature and density show that for the fixed density of evaporated atoms, clusters become smaller at higher temperature T_0.

(4) We demonstrate the possibility of oscillation phenomena in condensation and we show that within some region of parameters these oscillations can produce clusters of different sizes.

ACKNOWLEDGMENTS

APPENDIX
Special Solution of Gas Dynamic Equations

The spherical plume expansion is described by solution of gas dynamics equations

$$\frac{\partial r}{\partial t} + \frac{1}{r^2}\frac{\partial}{\partial r}\left(r^2 rv\right) = 0, \tag{A.1}$$

$$\frac{\partial v}{\partial t} + v\frac{\partial v}{\partial r} + \frac{1}{r}\frac{\partial P}{\partial r} = 0, \tag{A.2}$$

$$\frac{\partial P}{\partial t} + v\frac{\partial P}{\partial r} + gP\frac{1}{r^2}\frac{\partial}{\partial r}\left(r^2 v\right) = 0, \tag{A.3}$$

where r, P and v are the density, pressure and velocity within the vapor, and $g = c_p/c_v = const$ is the adiabatic exponent.

The self-similar isentropic solutions are sought in the following form (see, e.g. [15])

$$v = r\frac{\dot{R}}{R}, \tag{A.4}$$

$$r = \frac{M}{I_1 R^3}\left[1 - \frac{r^2}{R^2}\right]^{\frac{1}{g-1}}, \tag{A.5}$$

$$P = \frac{E}{I_2 R^3}\left(\frac{R_0}{R}\right)^{3(g-1)}\left[1 - \frac{r^2}{R^2}\right]^{\frac{g}{g-1}}, \tag{A.6}$$

where normalization constants $I_1 = I_1(g)$ and $I_2 = I_2(g)$ are determined from the conditions of mass M and energy E conservation,

$$I_1 = \frac{p^{3/2} G\left(\frac{g}{g-1}\right)}{G\left(\frac{g}{g-1}+\frac{3}{2}\right)}, \quad I_2 = \frac{p^{3/2}}{g-1}\frac{G\left(\frac{g}{g-1}+1\right)}{G\left(\frac{g}{g-1}+\frac{5}{2}\right)}, \tag{A.7}$$

where $\Gamma(x)$ is the gamma-function [25].

Substituting the distributions (A.4) - (A.6) into the set of gas dynamic equations, one can easily find that the con-tinuity equation (A.1), as well as the entropy conserva-tion equation (A.3), are fulfilled identically. The Euler's equation (A.2) is transformed into an

ordinary differential equation which describes the motion law for expanding plume boundary

$$\frac{d^2R}{dt^2} = (5g - 3)\frac{E}{M}\frac{1}{R}\left(\frac{R_0}{R}\right)^{3(g-1)}, \tag{A.8}$$

$$R\big|_{t=0} = R_0, \qquad \frac{dR}{dt}\big|_{t=0} = u_0.$$

The first integral of this equation is similar to energy conservation law in classical mechanics

$$\left(\frac{dR}{dt}\right)^2 = u_0^2 + \frac{2}{3}\left(\frac{5g-3}{g-1}\right)\frac{E}{M}\left[1 - \left(\frac{R_0}{R}\right)^{3(g-1)}\right]. \tag{A.9}$$

The further integration of this equation yields the solution in the form of inverse function $t = t(R)$. This solution is represented through the hypergeometric function $_2F_1(a, b; c; z)$ [25], where parameters a, b and c are

$$a = \frac{1}{2}, \quad b = -\frac{1}{3(g-1)}, \quad c = 1 - \frac{1}{3(g-1)}. \tag{A.10}$$

The final formula is given by

$$t^* = \left[u^{*2} + \frac{2}{3(g-1)}\right]^{-\frac{1}{2}}$$

$$\times \left\{R^* \cdot _2F_1\left[a,b;c;\frac{R^{*-3(g-1)}}{1+\frac{3}{2}(g-1)u^{*2}}\right]\right.$$

$$\left. - _2F_1\left[a,b;c;\frac{1}{1+\frac{3}{2}(g-1)u^{*2}}\right]\right\}. \tag{A.11}$$

Here we used the nondimension variables

$$t^* = \frac{t}{t_0}, \quad t_0 = R_0\sqrt{\frac{1}{5g-3}\frac{M}{E}},$$

$$R^* = \frac{R}{R_0}, \quad u^* = \frac{u_0 t_0}{R_0}. \tag{A.12}$$

The function $t^* = t^*(R^*)$ depends on two parameters: the adiabatic exponent, g, and the initial velocity of plume expansion, u^*. The behavior of this function is shown in Fig. 7.

It is easy to see directly from (A.9) that the velocity of expansion tends to constant $dR/dt \rightarrow u_\infty$ for sufficiently extended time (inertial stage of expansion), where

$$u_\infty^2 = u_0^2 + \frac{2}{3}\frac{5g-3}{g-1}\frac{E}{M}. \tag{A.13}$$
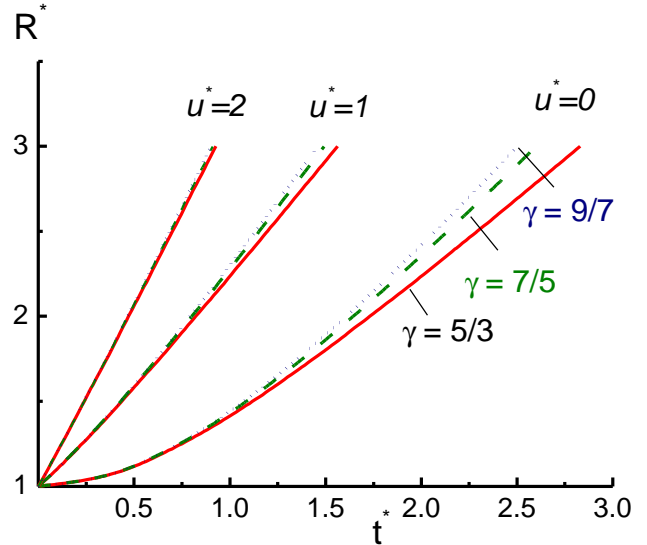
Fig. A.1. The dependencies $R^* = R^*(t^*)$ for different values of parameters g and u^* (according to (A.11)). Three curves with $g = 5/3$ (solid), $7/5$ (dash) and $9/7$ (dots) are shown for three values of velocity $u^* = 0, 1, 2$.

For the particular case $g = 5/3$ from (A.11) a simple formula which has been used in calculations follows:

$$\left(\frac{R}{R_0}\right)^2 = Y(t) \equiv$$

$$1 + 2\frac{u_0}{R_0}t + \left[\left(\frac{u_0}{R_0}\right)^2 + \frac{16}{3}\frac{E}{MR_0^2}\right]t^2. \tag{A.14}$$

REFERENCES

1. 1994, *Clusters of Atoms and Molecules.* Springer Series in Chemical Physics, vol. **52**, Haberland, H. Ed. (Berlin: Springer).
2. Melinon, P., Paillard, V., Dupuis, V., *et al.,* 1995, *Int. J. Mod. Phys. B,* **9**, 339.
3. Smirnov, B. M., 1994, *Usp. Fiz. Nauk*, **164**, 1165; **164**, 665.
4. Marine, W., Movtchan, I., Simakine, A., *et al.*, 1996, *Mat. Res. Soc. Symp. Proc.*, Singh, R., Norton, D., Laude, L., *et al.*, Eds. (Pittsburg) **397**, 365
5. van de Riet, E., Nillesen, C. J. C. M., and Dieleman, J., 1993, *J. Appl. Phys.* **74**, 2008.
6. Yoshida, T., Takeyama, S., Yamada, Y., and Mutoh, K., 1996, *Appl. Phys. Lett.* **68**, 1772.
7. Callies, G., Schittenhelm, H., Berger, P., and Hüdel, H., 1997, Abstracts of EUROMECH Colloquium 363 "*Mechanics of Laser Ablation*", Novosibirsk, 11.
8. Lifshitz, E. M. and Pitaevsky, L. P., 1979, *Physical Kinetics*, (Moscow, Nauka) (in Russian).
9. Bäuerle, D., 1996, *Laser Processing and Chemistry*, 2nd ed. (Berlin: Springer)
10. Zeldovich, Ya. B., 1942, *Sov.Phys. JETP*, **12**, 525.
11. Raizer, Yu. P., 1960, *Sov. Phys. JETP*, **37**, 1229.
12. Zeldovich, Ya. B. and Raizer, Yu. P., 1966, *Physics of Shock Waves and High - Temperature Hydrodynamic Phenomena*, (New York: Academic).

13. Frenkel, Ya. I., 1945, *Kinetic Theory of Liquids,* (Moscow: Acad. Sci.).

14. Ehbrecht, M., Ferkel, H., Holz, L., *et al.*, 1995, *J. Appl. Phys.*, **78**.

15. Anisimov, S., Bäuerle, D., Luk´yanchuk, B., 1993, *Phys. Rev. B* **48**, 12076.

16. Landau L. D., Lifshitz E. M., 1976, *Statistical Physics*, (Moscow: Nauka) (in Russian) Part 1.

17. 1972, *American Institute of Physics Handbook*, 3rd ed., Gray D. E. Ed. (New York: McGraw-Hill).

18. Santis, M., Patrone, L., Luk'yanchuk, B., *et al. to be published*.

19. Anisimov, S. I., and Khokhlov, V. F., 1995, *Instabilities in Laser-Matter Interaction*, (London: CRC).

20. Karlov, N. V., Kirichenko, N. A., and Luk'yanchuk B. S., 1997 *Laser Thermochemistry. Fundamentals and Applications,* (Cambridge: Cambridge Interscience Press).

21. Hirschfelder, J. O., Curtiss, C. E., and Bird, R. B., 1967, *Molecular Theory of Gases and Liquids*, (New York, John Willey & Sons).

22. Wolfram, S., 1991, *Mathematica*, 2nd ed., (Addisson-Wesley).

23. Hubmer, G. B., and Titulaer, U. M., 1990, *J. Stat. Phys.*, **59**, 441; 1991, **63**, 203.

24. Anisimov, S., Luk´yanchuk, B., and Luches, A., 1996, *Appl. Surf. Sci.*, **96 - 98**, 24.

25. Gradshteyn, I. S., Ryzhik, I. M., 1957, *Table of Integrals, Series, and Products,* (New York: Academic Press).